

Predicting Eccentric Stresses for Large Diameter Open Ended Pipe Piles

Scott Webster, P.E.,¹ Brent Robinson, PhD, P.E.², Ryan Allin, P.E.,³ and
Rory Flynn, P.E.⁴

¹GRL Engineers, Inc., 4350 Main Street, Suite 211, Harrisburg, NC 28075; E-mail:
Swebster@grlengineers.com

²Pile Dynamics, Inc. 30725 Aurora Road, Cleveland, Ohio 44139; E-mail: Brobinson@pile.com

³Pile Dynamics, Inc. 30725 Aurora Road, Cleveland, Ohio 44139; E-mail: Rallin@pile.com

⁴GRL Engineers, Inc. 6677 Lincoln Ave., Suite 333, Lincolnwood, IL 60712; E-mail:
Rflynn@grlengineers.com

ABSTRACT

Recent experience with dynamic pile testing results of Large Diameter Open Ended Pipe piles (LDOEP) has provided some insight to consider when such piles need to penetrate very dense soil or rock layers. In soil conditions where these piles need to penetrate such layers to achieve sufficient geotechnical resistance or fulfill lateral stability requirements, the potential for pile damage needs to be assessed. In addition to potential uniform compression stress at or near the pile toe, consideration should also be given to possible eccentric compression stress. The uniform pile toe compression stresses can be evaluated by wave equation results during the design phase of the foundations. Then, the design team can consider alternate pile diameters and wall thickness to prevent over stressing of the pile toe. During pile installations, dynamic pile monitoring can calculate the pile toe stress based upon the Case Method equations. CAPWAP analysis can further refine the calculation and location of the maximum compression stress. However, none of these methods can directly assess eccentric stresses which might occur where the pile toe encounters the dense soil or rock layer at an angle due to pile batter or sloping soil/rock layer. The paper will present examples where such stresses were encountered, and pile damage was apparent. Based upon the pile monitoring results and the evident pile damage encountered a method to calculate the apparent eccentric stresses is provided. The method proposed would be used in combination with wave equation or dynamic monitoring results to predict the combination of uniform dynamic and eccentric stress for piles driven at an angle or to soil layers with an expected slope.

INTRODUCTION

Dynamic pile testing of driven pile foundations was developed by a research project at Case Western Reserve University (Goble et al., 1975). The original research project goal was to develop a system to replace static pile load testing by performing dynamic pile testing using the Pile Driving Analyzer® (PDA). This system uses strain and acceleration measurements from

reusable sensors to assess three primary results, geotechnical resistance at the time of testing, transferred hammer energy and dynamic driving stresses. These results were established using the closed form solutions called Case Method and by signal matching using the numerical model called CAPWAP® (Rausche et al., 1972). Over the decades numerous correlations have been performed by multiple entities between dynamic and static load testing results. These correlations have provided generally good agreement between the two methods (Likins and Rausche, 2004).

While most of the current practice of dynamic pile testing focuses on pile geotechnical resistance and a resulting driving criterion for production piles, the testing may also provide an assessment of the pile integrity. Early test results noted that H piles driven to end bearing on rock appeared to occasionally have an unexpected result. The early research noted “If the velocity increases sharply relative to the force at any point earlier than the $2L/c$ time it indicates damage has weakened the pile” (Goble et al. 1977). These test piles were extracted and visual inspection confirm that pile damage had occurred. Figure 1 shows a typical damaged pile encountered during the original research effort.



Figure 1. Damaged H pile.

Allowable Driving Stresses

Based upon these results it was clear that establishment of allowable driving stresses was needed to prevent or limit piles being damaged during driving. Based upon years of experience allowable driving stresses have been developed for various pile types. These allowable driving stresses are based upon the pile material strength. Therefore, allowable stresses are determined based upon the yield stress of the steel for steel piles, the concrete strength and effective pre-

stress, if any, for concrete piles. Typical limits are proposed by AASHTO (2010) and FHWA Design and Construction of Driven Pile Foundations (2016) and have been similarly adopted by many other international codes and standards:

- 90% of the steel yield strength for steel piles in either compression or tension
- 85% of the concrete compressive strength minus the effective prestress for concrete piles in compression, and
- 100% of the effective prestress plus an allowance for the concrete's tensile strength which is typically 1.4 to 2.1 MPa (0.2 to 0.3 ksi) for prestressed concrete piles in tension.

Dynamic pile testing for the past several decades has been used to determine driving procedures that will maintain pile driving stresses below the above recommended limits. These procedures would specify the maximum hammer energy, stroke, or fuel setting with a blow count criterion. As an example, to limit tension stresses for concrete piles the hammer energy (stroke) is often reduced during low blow counts to avoid excessive tension stresses. Limiting compression stresses may conversely be controlled by limiting the hammer energy (stroke) at high blow counts.

The β -Method

The β -Method looks for tension reflections caused by reduced cross section or material strength along the pile length. The maximum local reduction in the upward wave from this early reflection is related to the extent of the pile damage. The local reflection caused by the damage along the pile can be computed as

$$\Delta = Z v(t_3) - F(t_3) + R \quad (1)$$

Where t_3 is a time (between initial impact and the reflection from the toe) of the local minimum in upward wave that corresponds to the damage and R is the total skin friction resistance, including dynamic resistance, above the damage location. Then based upon wave theory, Rausche and Goble (1979) showed that

$$\alpha = 0.5 \Delta / (F(t_1) - R) \quad (2)$$

Where t_1 is the time of the initial force input peak and α can be used to quantify the section reduction by inclusion in the expression

$$\beta = (1 - \alpha) / (1 + \alpha) = Z_2 / Z_1 \quad (3)$$

Where Z_1 is the undamaged pile impedance and Z_2 is the impedance for the damaged pile section. As such the β value is expressed as a percentage of the remaining impedance section

compared to the original pile impedance. Normally there will not be a change in the pile material so the expected change would be anticipated to be a difference in cross section.

In most cases where pile damage occurs the normal cause is that the encountered driving stresses exceed the pile strength. This is common for concrete or timber piles where the piles strengths are relatively low while the potential for excessive driving stresses is quite high. However, this may not always be the case as has been experienced for piles driven to dense sand and rock formations. Under these conditions the average stress across the pile section may be measured to be within the allowable limits but pile damage has still occurred. Pile damage is encountered as the concentrated stress at the critical location has exceeded the pile strength. These conditions have often been encountered for steel H piles or open ended pipe piles driven to very strong sand or rock formations. Dynamic monitoring shows the pile top and pile toe stresses to be within allowable limits but pile damage has still occurred. This is often due to the pile toe encountering these dense formations with only part of the cross sectional area, resulting in a concentrated or eccentric stress.

Estimating Eccentric Stresses

Large diameter open ended pipe (LDOEP) piles are inferred to encounter eccentric stresses where the piles are driven into very dense sands or rock formations. This typically occurs for piles driven on a batter angle and where shallow dense formations are present within the subsurface geology. The pile toe would be expected to contact the dense layer on one side of the pile, while the opposite side remains above the dense layer. The authors have performed numerous driveability analyses for projects which have encountered these conditions. As a part of these studies an estimate of the potential eccentric driving stress has been calculated. For these studies it was assumed that the soil resistance at the toe would have an eccentricity of approximately one half the inner radius of the LDOEP. The eccentric force generates a moment in the pile equal to:

$$M = d (F) \quad (4)$$

Where d is the distance between the center of the pile and the reaction (an eccentricity value), and F is the force in the pile (at or near the pile toe) resulting from a concentrated geotechnical resistance from the rock or dense soil, generating a stress increase of:

$$\Delta\sigma = M r / I \quad (5)$$

Where $\Delta\sigma$ is the increase in the stress, r is the pipe's inner radius and I is the ring moment of inertia. This calculation requires an assumption of the eccentricity, d , at which the applied force on the pile toe acts. The authors have generally assumed an eccentricity of one half the inner radius of the pile for scenarios where potential for tip damage is suspected.

To further assess the assumption of the applied force eccentricity (one half inner radius) the authors have taken two examples where pile damage was indicated and confirmed to have occurred. At both locations multiple LDOEP piles were driven and tested using the PDA® system. Measurements of strain and acceleration were collected and analyzed to assess apparent pile stress conditions while driving into or through a known dense layer. Based upon the measured or calculated average stresses the increase in stress due to the eccentric force could be calculated and thus the apparent force eccentricity was determined.

CASE HISTORY

Example 1 – Shallow Rock Layer

The first example was a project that required piles to penetrate a “weak” rock layer between 4.2 and 9.9 meters below the mudline. The piles for this project were 1067 mm diameter with a wall thickness of 38.1 mm which increased to 44.5 mm over the final 2.9 meters. The piles were fabricated with steel having a minimum yield strength of 345 MPa. The site is well known for having variable shallow “weak to moderately strong” rock layers and the potential for pile refusal is often difficult to impossible to predict. Table 1 provides the general soil stratigraphy:

Layer	Depth Range (m)	Description
1	0.0 to 1.2	Clayey silica SAND
2	1.2 to 4.2	Soft to very stiff fat CLAY
3	4.2 to 9.9	Moderately weak to moderately strong slightly weathered GYPSUM
4	9.9 to 12.3	Hard to very hard slightly cemented fat CLAY
5	12.3 to 14.5	Moderately weak to moderately strong slightly weathered GYPSUM
6	14.5 to 28.5	Hard to very hard slightly to moderately cemented fat CLAY
7	25.8 to 32.8	Weak to moderately strong weathered GYPSUM

Table 1 – General soil profile Example 1

Unfortunately for this site very limited information was provided as to the strength of the rock layers. Thus, preconstruction driveability analyses did not predict refusal driving conditions for the above layers. However, it should be noted that prediction of refusal driving conditions is very difficult for this soil stratigraphy.

Four foundation piles were driven for this project with planned pile penetrations ranging from 29 to 64 meters. All piles were driven on a batter angle of 1H:17V or 3.37 degrees. Thus, the piles would need to penetrate the shallow rock layers indicated above and it could be assumed that the pile batter would result in an eccentric force at or near the pile toe. In fact, preconstruction wave

equation analyses were performed and calculations for the predicted eccentric stresses were provided as per equations 4 and 5 above. The eccentric force was assumed to have an eccentricity of 0.245 meters or one half the pile inner radius. Based upon the analysis the increase in stress due to the eccentric loading at the pile toe was calculated to range from 141 to 171 MPa. This eccentric stress was added to the predicted axial stress which resulted on the combined predicted stress ranging from approximately 282 to 341 MPa. It should be noted that reduced hammer energies while driving through these layers was recommended to avoid overstressing of the pipe piles.

All four foundation piles experienced hard driving and refusal blow counts at pile penetrations of 4.9 to 5.6 meters. In an effort to drive the piles through the rock layer, the first pile driven experienced higher blow counts and more hammer blows at slightly higher hammer energies (and therefore higher pile stresses) than the remaining three piles. Upon completion of the driving, it was decided that drilling out the piles and through the rock layer would be performed to advance the piles. During drilling operations, it was discovered that the first pile driven was obstructed near the pile toe while the remaining three piles were drilled as planned beyond the rock layer. It was suspected that the first pile's toe may have collapsed, preventing the drilling to proceed beyond the pile toe. To confirm this suspicion, the pile was extracted for visual inspection. Figure 2 shows the suspected pile toe damage.



Figure 2 – Pile toe damage

CAPWAP analysis performed on dynamic pile testing data indicated that the pile toe stresses for the four piles were 261, 253, 219 and 194 MPa. If the eccentric stress is calculated as having an eccentricity of one half the inner radius (0.245 meters) and using the pile toe force from the CAPWAP analyses, then the combined stresses would be 589, 503, 436 and 390 MPa, respectively. As such, the increase in stress due to the eccentric force could not be this high or all four piles would have experienced some pile damage. If the eccentric stress is calculated using an eccentricity of one fifth (1/5) of the inner pile radius (0.098 meters) then the resulting combined stresses would be 392, 352, 306 and 271 MPa. The highest calculated stress was indicated for the pile which encountered the pile toe damage. Only one other pile indicated a combined stress greater than the pile yield strength of 345 MPa and this combined stress was only slightly greater than the yield strength (352 MPa vs. 345 MPa). This pile likely did not yield as the indicated stress was not applied for a significant number of hammer blows or the pile actual yield strength was greater than the minimum yield strength.

Example 2 – Weak Limestone Moderate Penetration

The second example was a project that required piles to penetrate numerous sand and clay layers followed by “weak” limestone or sandstone layers between 26.0 and 63.0 meters below the mudline. The piles for this project were 1067 mm diameter with a wall thickness of 44.5 mm which increased to 50.8 mm over the final 2.9 meters. The piles were fabricated with steel having a minimum yield strength of 345 MPa. The site is known for having the potential for hard driving and occasional refusal driving conditions. Table 2 provides the general soil stratigraphy:

Layer	Depth Range (m)	Description
1	0.0 to 0.4	Dense to very dense silty siliceous SAND
2	0.4 to 1.6	Loose to medium dense clayey siliceous SAND
3	1.6 to 4.8	Medium dense to dense silty siliceous SAND
4	4.8 to 6.0	Very dense siliceous SAND
5	6.0 to 6.6	Hard sandy carbonate SAND
6	6.6 to 11.6	Very dense locally weakly cemented silty fine siliceous SAND
7	11.6 to 15.85	Dense to very dense locally weakly cemented silty siliceous SAND
8	15.85 to 16.35	Cemented silty siliceous SAND
9	16.35 to 18.8	Weakly to moderately cemented silty siliceous SAND
10	18.8 to 20.6	Very weak to weak siliceous CALCARENITE
11	20.6 to 21.55	Locally weakly cemented very clayey SAND
12	21.55 to 24.35	Extremely weak to very weak siliceous CALCARENITE
13	24.35 to 26.0	Hard weakly cemented sandy CLAY/SILT
14	26.0 to 27.7	Weak fine grained siliceous LIMESTONE

Layer	Depth Range (m)	Description
15	27.7 to 31.0	Very weak calcareous SANDSTONE
16	31.0 to 38.0	Very weak to weak calcareous SANDSTONE
17	38.0 to 40.0	Extremely weak to very weak calcareous SANDSTONE
18	40.0 to 43.7	Very weak calcareous SANDSTONE
19	43.7 to 49.0	Very weak to weak calcareous SANDSTONE
20	49.0 to 52.0	Very weak calcareous SILTSTONE
21	52.0 to 56.0	Very weak to weak siliceous CALCISILTITE
22	56.0 to 60.0	Extremely weak to very weak calcareous SILTSTONE
23	60.0 to 61.75	Weak calcareous SANDSTONE
24	61.75 to 68.15	Very weak to weak calcareous SILTSTONE

Table 2 – General soil profile Example 2

The geotechnical report for this site provided extensive strength parameters for the cemented sand and weak rock layers. Numerous unconfined compression tests, point load tests and extensive coring data including core recovery and rock quality designation (RQD) were provided. Preconstruction driveability analyses were based upon the expected static pile geotechnical resistance calculations and did not predict refusal driving conditions for the cemented sand or weak rock layers. However, refusal driving was considered possible or even likely based upon the thickness of the rock layers and the relatively high RQD values (50 to 100) obtained during the soil sampling and coring.

Four foundation piles were driven for this project with planned pile penetrations ranging from 26.5 to 63 meters. All piles were driven on a batter angle of 1H:17V or 3.37 degrees. Thus, the piles would need to penetrate the calcarenite, limestone and sandstone layers indicated above and it could be assumed that the pile batter would result in an eccentric force at or near the pile toe.

Two of the four piles experienced refusal driving conditions at depths of approximately 25.25 and 28.5 meters. These depths correspond to the approximate depths of the limestone and sandstone layers where UCS strengths were notably greater (ranged from 8 to 26 MPa) and the RQD values were reported to be 100%. Thus, the rock layers at this depth encountered in the investigation and by the piles were clearly much stronger. The reported pile driving blow counts were 212 and 312 blows per 0.25 meter at respective pile penetrations of 28.5 and 25.25 meters. The pile with the higher blow count (312/0.25m) was declared at the time of driving to have reached refusal and driving was halted. The pile with the lower blow count (212/0.25m) was determined to have been damaged approximately 4 meters above the toe.

The apparent pile damage was indicated by the dynamic pile testing force and velocity records as shown in Figure 3 below. It should not be considered unexpected that the pile damage was indicated approximately 4 meters above the pile toe. In fact, this location would generally be

considered the critical pile section since an increase in pile cross section occurs 2.9 meters above the pile toe. The increase cross sectional area will result in stress concentrations just above the interface, in the thinner section, as per stress wave theory. The combination of increased axial stress and potential increase in eccentric stress should be considered prior to pile installation.

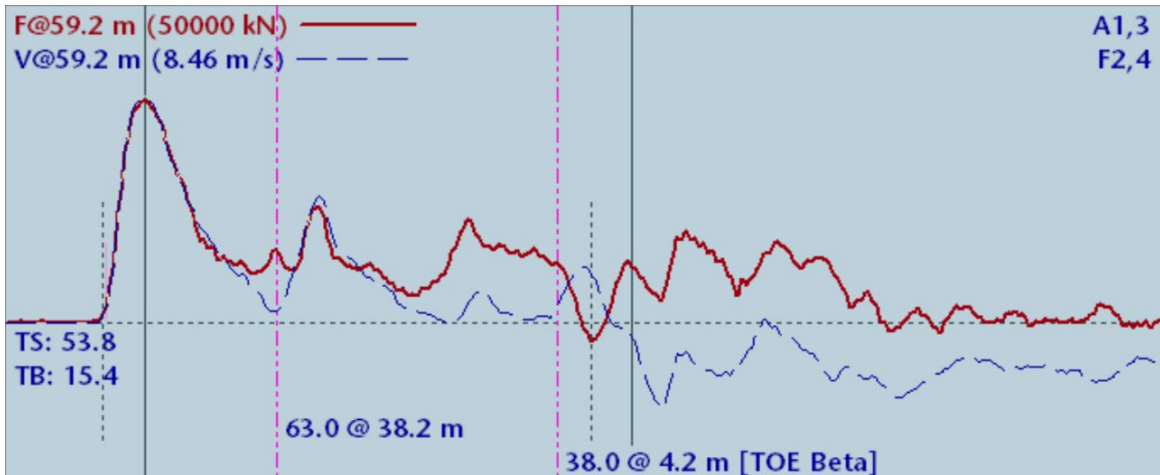


Figure 3 – Representative force and velocity plot indicating damage 4.2 meters above toe.

CAPWAP analysis performed on dynamic pile testing data indicated that the axial compression stress was 233 MPa approximately 3 meters above the pile toe and 227 MPa at the pile toe. This is consistent with stress wave theory and the expected results. If the eccentric stress is calculated using an eccentricity of one fifth (1/5) of the inner pile radius (0.098 meters) then the resulting combined stress 3 meters above the pile toe would be 324 MPa for the pile which was indicated to have pile damage. Thus, in this case it is likely that the eccentric stress is due to an eccentricity greater than one fifth of the inner pile radius. Using an eccentricity of one fourth the radius results in a calculated combined stress of 347 MPa. For the second pile which encountered refusal driving the calculated stress would be 279 MPa using an eccentricity of one fourth the inner pile radius.

CONCLUSIONS

Based upon the examples above, one should consider the potential for LDOEP piles to experience higher compression stresses should the piles encounter rock or very dense cemented sand layers where only a portion of the pile toe will be in contact with the layer. This will occur for planned batter pile foundations or due to sloping rock/sand layers. The authors have been involved with numerous projects where the potential for over stressing of LDOEP piles was present. Typically, these conditions have been assessed by preconstruction driveability analyses and estimation of the potential eccentric stress. Until recently the eccentric stress has been estimated as having an eccentricity of one half (1/2) the inner pile radius at the critical cross section. This assumed eccentricity has often resulted in the requirement that significantly

reduced hammer energies be used when driving through these layers. Thus, pile refusal would often be predicted or considered highly likely.

The two examples presented appear to indicate that the eccentricity for these two similar projects was approximately one fifth (1/5) to one fourth (1/4) of the inner pile radius. Of course, for these projects pile damage was encountered which was either visually confirmed or very clear from the dynamic pile testing data. Therefore, the authors would recommend that a minimum eccentricity of one fourth (1/4) to one third (1/3) of the inner pile radius be used for preconstruction driveability analysis and estimation of the compression stresses including the eccentric stress at the pile toe or just above the pile toe. However, it should be noted that these piles had a small batter angle (1H:17V) and therefore, piles with steeper batters or large rock slopes may require higher eccentricity for calculation of the additional stress. The same condition may be true for larger diameter piles although this should be somewhat accounted for in the use of a percentage of the pile radius for the calculation of the eccentric stress.

REFERENCES

- AASHTO. (2010). "LRFD Bridge Design Specification". *5th Edition, American Association of State Highway and Transportation Officials*, Washington D.C.
- FHWA. Geotechnical Circular No. 12, Design and Construction of Driven Pile Foundations, Volumes 1 and II. *GEC 12: Report FHWA-NHI-16-010, US Department of Transportation, FHWA*, Washington DC; 2016.
- Goble, G. G. Likins, G. E., Rausche, F. (1975). "Bearing Capacity of Piles from Dynamic Measurements", *Final Report, Ohio Department of Transportation*, Cleveland, OH.
- Goble, G. G. Likins, G. E., Teferra, W. (1977), "Piles and Pile Driving Hammer Performance for H-piles Driving to Bedrock", *Ohio Department of Transportation and Federal Highway Administration*. Cleveland, OH.
- Likins, G. E. and Rausche, F. (2004). "Correlation of CAPWAP with Static Load Tests", *Proc. Of the 7th Int Conf. on the Application of Stresswave Theory to Piles*. Petaling Jaya, Malaysia, 153-165.
- Rausche, F, Moses, F., Goble, G.G. (1972). "Soil Resistance Predictions From Pile Dynamics". *Journal of the Soil Mechanics and Foundations Division, American Society of Civil Engineers*. Vol 98, SM9, Proc. Paper 9220, September, 1972.